RESEARCH ARTICLE

Editorial Process: Submission:11/10/2024 Acceptance:08/10/2025 Published:08/22/2025

Matairesinol Targets Lipid Metabolism Reprogramming in AR-Independent Prostate Cancer Cells

Minal Mahajan[1], Gauri Ghodke[2], Manali Joshi[2], Amol Chaudhary[1], Ruchika Kaul-Ghanekar[1,3,4]*

Abstract

Objective: Metabolic reprogramming, especially lipid reprogramming, is critical in cancer progression, including prostate cancer (PCa). Androgen deprivation therapy (ADT) is commonly used to slow down tumor spread and Lipid metabolism has been linked to its resistance in PCa. This study examines the therapeutic potential of Matairesinol (MA), a plant-derived lignan, in targeting lipid reprogramming in PCa cells. **Methods:** PC-3 cells were treated with different doses of MA and its effect was studied on cell growth and induction of apoptosis by trypan blue dye exclusion and JC-1 dye assays, respectively. The altered expression of *de novo* fatty acid, cholesterol biosynthesis and other associated genes were evaluated by qPCR. Changes in intracellular lipid accumulation were assessed by Nile red staining. The bioinformatics approach was used to identify the main targets of MA using DrugBank, PubChem, and BindingDB databases, and molecular docking was performed with Autodock 4.2 to predict the binding of MA. **Results:** MA significantly impaired PCa cell growth and mitochondrial membrane potential, inducing apoptosis. MA modulated mRNA expression of fatty acid and cholesterol biosynthesis, lipid transport, and lipolysis-related genes, and reduced lipid accumulation. Bioinformatics analysis with DrugBank, PubChem, and BindingDB revealed the main targets of MA; and molecular docking with AutoDock 4.2 predicted MA binding and identified SHBG and DHRS4L2 as potential targets. *In vitro* validation confirmed that MA significantly reduced mRNA levels of SHBG and DHRS4L2 in PC-3 cell line. **Conclusion:** By targeting lipid metabolism, MA holds promising potential as a therapeutic agent for PCa, especially in ADT-resistant and Metastatic Castration Resistant Prostate Cancer (mCRPC) cases.

Keywords: PC3 cell line- bioinformatics- apoptosis- lipid regulation- SHBG- DHRS4L2

Asian Pac J Cancer Prev, **26 (8)**, 2855-2867

Introduction

Prostate cancer, responsible for around 15% of cancer cases in men, is the most prevalent cancer in 112 countries as of 2020, the second most diagnosed globally, and the fifth leading cause of cancer-related deaths, with a mortality rate of 6.8% [1-3]. The Lancet Commission predicts that the annual number of new prostate cancer cases will increase from 1.4 million in 2020 to 2.9 million globally by 2040 [2]. In India, PCa ranks third among the cancer sites observed in males with a cumulative risk of 1 in 125 men [4]. Although prostate cancer is reported to be less prevalent in India compared to Western countries [2], recent data from 25 population-based the cancer registries in India show a rise in prostate cancer incidence [5]. In India, prostate cancer is often diagnosed at late stages, with 85% of patients diagnosed at Stage III-IV compared to only 15% in the USA [6]. Among Indian migrants to America, the incidence of pT3 Prostate cancer, seminal vesicle extension, and mortality is notably higher than in Caucasians [7, 8].

In terms of treatment, only localized and loco-regional prostate cancer (often termed Castration-Sensitive Prostate Cancer-CSPC) is potentially curable, whereas distant metastasis to bone or soft tissue (often termed Castration-Resistant Prostate Cancer-CRPC) renders it incurable with current therapeutics [2, 9]. Although non-metastatic prostate cancer (M0 PCa) has an excellent prognosis, the 5-year survival rate rapidly drops to just 31% when it advances to a metastatic stage (M1 PCa) [10]. Prostatectomy and radiotherapy remain mainstay therapeutic options for CSPCs (Castration-Sensitive Prostate Cancers) [10]. For non-metastatic Castration-Resistant Prostate Cancers (nmCRPCs), which develop from localized tumors, treatment includes use of Androgen Pathway Inhibitors (APIs). Although Prostatectomy, APIs

*[1]Cancer Research Lab, Interactive Research School for Health Affairs (IRSHA), Bharati Vidyapeeth (Deemed to be University), Pune-Satara Road, Pune-411043, Maharashtra, India. [2]Bioinformatics Center, Savitribai Phule Pune University, Pune, Maharashtra, India. [3]Symbiosis Centre for Innovation and Research (SCRI); Symbiosis International Deemed University (SIU), Pune, Maharashtra, India. [4]Cancer Research Lab, Symbiosis School of Biological Sciences (SSBS), Symbiosis International Deemed University (SIU), Pune, Maharashtra, India. *For Correspondence: ruchika.kaulghanekar@gmail.com*

(such as enzalutamide), and ADT have been shown to improve survival and quality of life in localized CSPCs, they lead to the development of nmCRPCs or metastatic CRPCs (mCRPCs) due to resistance [8, 11]. In contrast, managing these advanced stages require a robust treatment regimen that includes Docetaxel, Cabazitaxel, APIs, and PARP inhibitors (PARPi) to slow the progression of PCa [9]. mCRPCs are typically highly aggressive, and exhibit resistence to existing standard treatment, with patients dying within 2-4 years [12-14]. Thus, there is an urgent need to investigate treatment options for mCRPCs [15].

Metabolic reprogramming in cancer progression is recognized as a one of the hallmarks cancer [16-18]. Lipid Metabolic Reprogramming (LMR) is implicated in many cancers including, metastatic PCa [14]. Progressively increasing rate of *de novo* fatty acid synthes is obesrved in PCa,which is at its peak [19-21]. A new strategy for treating mCRPC involves inhibiting ACC1 and blocking exogenous fatty acid uptake to prevent cancer cells from compensating for reduced lipogenesis [22, 23]. Single-cell RNA sequencing of mCRPC tumors has shown SREBPs as crucial targets, with their inhibition resulting into regulation of PC3 cell growth [24]. Clinical data has shown that PPARγ levels increase with the progression of PCa which may become reliant on PPARγ for lipogenesis and mitochondrial biogenesis [25]. Therefore, targeting PPARγ could be a promising therapeutic strategy for preventing the development of PCa. Suppressing fatty acid uptake, mediated through CD36 (usually gained or amplified), has shown therapeutic effect in preclinical models of PCa [26]. PPARγ promotes PCa by activating lipid signaling pathways, which include *de novo* fatty acid and cholesterol production, lipid transport, and lipid breakdown through both androgen receptor-dependent and independent mechanisms [25]. Around 27% of patients with castration-resistant PCa, amplification and overexpression of PPARγ gene, particularly in AR-negative cell lines such as DU145 and PC-3 [27], has been obesrved. Gene expression analysis shows that ACLY, ACC, and FASN are significantly elevated in the PCa compared to the normal prostate tissue [21]. Inhibiting FASN reduces intracellular *de novo* fatty acids and causes malonyl-CoA build up, which inhibits fatty acid oxidation by blocking CPT1 [28]. Moreover, the genetic deletion of FASN reduces the invasive potential of PCa driven by of PTEN loss [29].

Lignans, the plant-derived polyphenolic compounds, exhibit anticancer activity by inhibiting cancer cell proliferation, inducing apoptosis, and reducing tumor angiogenesis and metastasis [30]. One of the plant-derived lignan-Matairesinol (MA), has been reported to exert cytotoxic activity against leukemia [31], breast [32, 33], pancreatic [34], and prostate cancers [35, 36]. MA has also exhibited anti-inflammatory [37], immunomodulatory [38], and anti-angiogenic [39] properties in a range of *in vitro* and / *in vivo* models. We have recently shown that MA reduced the viability of breast and prostate cancer cell lines and regulated Histone Deacetylase 8 (HDAC8) activity [40]. Recently, MA nanoparticles have been shown to restore chemosensitivity of colorectal cancer preclinical models by lipid reprogramming [41]. While MA has demonstrated anti-cancer activity against various cancers, its potential to target lipid reprogramming in PCa remains unexplored. In the present study, we have elucidated the therapeutic potential of MA in both in vitro (Pca cell line,PC3) and in silico model. From this integrated approach, we found that MA induced lipid reprogramming in the PC3 prostate cancer model (CRPC) and led to apoptosis.

Materials and Methods

Chemicals and reagents

Fetal bovine serum (FBS), Ham's F12 nutrient mix, streptomycin, and penicillin were procured from Gibco (USA). Matairesinol (HPLC grade, purity ≥85 %), Glutamine, Carbonyl cyanide 4-(trifluoromethoxy) phenylhydrazone (FCCP), 5,5′,6,6′-Tetrachloro-1,1′,3,3′ tetraethyl-imidacarbocyanine iodide (JC1), Fatostatin and KiCqStart™ primers were purchased from Sigma-Aldrich (USA). Nile red, TRI Reagent™, dNTP mix, Oligo(dT), RNaseOUT™, and DTT were purchased from Invitrogen (USA). M-MuLV Reverse Dithiothreitol Transcriptase was procured from Genei, India. TB Green Premix Ex Taq II (Tli RNaseH Plus). qPCR Master Mix was procured from Takara, Japan. Trypsin 0.25% Solution and all other common reagents were procured from HiMedia, India. Cell-culture and molecular biology grade plasticware were purchased from Eppendorf (Germany).

Cell culture

The PC-3 cell line, a poorly differentiated AR-negative mCRPC model [42, 43], was obtained from the National Centre for Cell Science (NCCS) in Pune, India. The cells were cultured in Ham's F12 nutrient mix, supplemented with 10% fetal bovine serum (FBS), 100 U/ml penicillin-streptomycin, and 2 mM L-glutamine. The culture was maintained in a humidified incubator at 37°C with 5% CO_2.

Cell growth/Trypan blue dye exclusion assay

The effect of MA on cell growth of PC-3 cells was evaluated by Trypan blue dye exclusion assay [44]. PC-3 Cells (1×10^5 cells/ml) were seeded in 24-well plates and incubated for 24h, followed by treatment PCa with different concentrations (0-200 μM) of MA for 24, 48, and 72 h. The cells were harvested, stained with Trypan Blue, and manually assessed for viability using a hemocytometer.

Mitochondrial membrane potential assay (Δψm)

The effect of MA on apoptosis of PC-3 cells was evaluated by using JC-1 dye as described previously [45]. Briefly, cells were seeded at a density of $1x10^4$ cells/well in a 96-black well plate for 24 h, followed by treatment with different concentrations (0-200 μM) of MA. FCCP (20 μM) was used as a positive control. Subsequently, JC-1 dye staining was performed on the PC3 cells. In brief, the cells were washed twice with 1X PBS and treated with 0.5 μg/ml JC-1 dye. They were then incubated in a CO2 incubator in the dark for 30 min. Following this, the cells were washed twice more with 1X PBS. After adding 100

µL of 1X PBS to each well, the fluorescence intensity was measured at 590/520 nm using a fluorescence microplate reader. Fluorescence readings were taken in a Fluostar Omega microplate reader (BMG Labtech), Germany at 520 nm (monomers) and 590 nm (J-aggregates). Values were expressed as the ratio of aggregate to monomer fluorescence intensity, normalized to the untreated cells.

Quantitative real-time PCR (qPCR)

Relative gene expression of genes involved in lipid reprogramming was evaluated in PC3 cells treated with MA (0-100 µM) for 24 h. Briefly, Total RNA was isolated from the untreated (C) and MA-treated PC-3 cells by using TRI Reagent® following the manufacturer's instructions. The 5 µg of total RNA was used for cDNA synthesis and subjected to qPCR analysis for evaluation of relative gene expression of genes at the mRNA level, using Kicqstart SYBR green primers on 7500-Fast Real-Time PCR System (Applied Biosystems™) (Table 1). qPCR conditions included initial denaturation for 30 s at 95°C, and 40 cycles, each consisting of 3 s at 95°C (denaturation), and 30 s at 60°C (annealing and extension) with extension optimum at 68°C. The relative mRNA expression levels for each target gene were calculated with β-actin as internal control using the $2^{-\Delta\Delta Ct}$ method [46].

Nile red staining

Nile red staining was performed to assess the effect of MA on intracellular lipid levels. For this cells were seeded at a density of 3 x 10^4 cells per well on coverslips in a 6-well plate and incubated overnight at 37°C with 5% CO_2. After 24 h, the cells were treated with varying concentrations of MA (0-100 µM), including a control group of untreated cells. The following day, the cells were washed with 0.1 M PBS (pH 7.4) and fixed with 10% formaldehyde in 0.1 M PBS (pH 7.4) for 15 min. The cells were then stained with Nile red solution (0.1 µg/ml in 150 mM NaCl) for 10 min at room temperature. Nuclei were counterstained with DAPI, and the coverslips were subsequently mounted onto glass slides for analysis. All microscopic fluorescent images were captured using the Olympus IX73 microscope (at 600X magnification) equipped with a Hamamatsu CMOS camera and its proprietary imaging software, CellSens (v 4.3).

Target Identification and Prediction of Ligand Binding Pose

Putative targets of MA were collected from BindingDB [47], PubChem [48], and DrugBank databases [49]. Standard Data File (SDF) was downloaded, and a canonical SMILES string (COC1=C(C=CC(=C1) CC2COC(=O)C2CC3=CC(=C(C=C3)O)OC)O) for MA (PubChem CID: 119205) was obtained and independently uploaded to the aforementioned servers. The default settings were used for all parameters. Consensus results pooled from the servers indicated two targets, Sex hormone-binding globulin (SHBG) and Dehydrogenase/ Reductase 4 Like 2 (DHRS4L2), henceforth referred to as DHRS4.

Molecular docking was performed using Autodock 4.2 [50] to predict the binding of MA with SHBG. Out of thirteen structures of SHBG at the Protein Data Bank (PDB), the entry, 6PYA [51], containing the protein with the ligand 3-[(1H-imidazol-1-yl) methyl]-2-phenyl-1H-indole and resolved at 1.71 Å, was chosen. This structure was chosen considering its higher resolution and co-crystallization with ligands somewhat similar in topology to MA. The protein was prepared by deleting all water

Table 1. List of KiCqStart™ Primers Used

S.N.	Gene	Sequence (5'à3')
1	*CYCS*	F- AAGAACAAAGGCATCATCTG
		R- GCTATTAAGTCTGCCCTTTC
2	*CASP9*	F- CTCTACTTTCCCAGGTTTTG
		R- TTTCACCGAAACAGCATTAG
3	*CASP3*	F- AAAGCACTGGAATGACATC
		R- CGCATCAATTCCACAATTTC
4	*PPARG*	F- AAAGAAGCCAACACTAAACC
		R- TGGTCATTTCGTTAAAGGC
5	*SREBF1*	F- AATCTGGGTTTTGTGTCTTC
		R- AAAAGTTGTGTACCTTGTGG
6	*ACC*	F- CAGTGAAGGCTTATGTTTGG
		R- CGTCATATGGATGATGGAATC
7	*ACLY*	F- GGTTCATTGGACACTATCTTG
		R- CGTCATATGGATGATGGAATC
8	*FASN*	F- CAATACAGATGGCTTCAAGG
		R- GATGTATTCAAATGACTCAGGG
9	*SCD*	F-CAGAGGAGGTACTACAAACC
		R- ATAAGGACGATATCCGAAGAG
10	*SREBF2*	F- CAGCAGGTCAATCATAAACTG
		R- GGACATTCTGATTAAAGTCCTC
11	*HMGCR*	F- ACTTCGTGTTCATGACTTTC
		R- GACATAATCATCTTGACCCTC
12	*LXR*	F- CATGACCGACTGATGTTC
		R- CAAACACTTGCTCTGAGTG
13	*ABCA1*	F- GTGTTTCTGGATGAACCC
		R- TTCCATTGACCATGATTGC
14	*ELOVL6*	F- AGTATATTCGGTGCTCTTCG
		R- TTAGCACAAATGCATAAGCC
15	*LIPE*	F- CTATGCTGGTGCAAAGAC
		R- CTCCAGGAAGGAGTTGAG
16	*ACSL1*	F- TGAGTGGGTGATTATTGAAC
		R- GTTGACTATGTACGTGATGG
17	*CPT1A*	F- ACGGGGATTATAAGTCAAGG
		R- CACAGCAAGTGAAAATCAAC
18	*SLC25A1*	F- ATGTTCGAGTTCCTCAGC
		R- ACTTCACCTTGATGGTCTC
19	*SHBG*	F- GACTCAGGCAGAATTCAATC
		R- AACACCACCTTTTGATCTTG
20	*DHRS4L2*	F- ATCGATATCCTAGTCTCCAATG
		R- TAATGTCCAGAGTCTTGTCC
21	*β-actin*	F-GATCAAGATCATTGCTCCTC
		R-TTGTCAAGAAAGGGTGTAAC

molecules and adding hydrogens as well as Gasteiger charges. The binding site of SHBG was defined based on the co-crystallized ligand. A grid box with dimensions 48 X 42 X 40 with a 0.375 Å spacing and center at -13.188, -23.564, and -7.570 Å was prepared. Docking runs (100) with a population size of 300 and 2,500,000 energy evaluations were performed with other algorithm parameters being kept as default. The pose with the lowest score was considered the best-docked pose.

The protein DHRS4 has only one entry in the PDB, 3O4R (unpublished), solved at a resolution of 1.7 Å. This entry is a complex of the protein and the cofactor NADP. The entry 2BGM [52], is a co-crystal structure of a related plant protein, secoisolariciresinol dehydrogenase with MA. The two proteins were superimposed and the coordinates of MA were copied from 2BGM to 3O4R. To refine the complex, the Standard Dynamics Cascade, in the absence of solvent, as implemented in Discovery Studio 2017, was implemented. Molecular Mechanics Force Field (MMFF) parameters were used for protein and ligand. This protocol includes energy minimization (1000 steps Steepest Descent (SD), 2000 steps Adopted Basis Newton-Raphson (ABNR)), stepwise heating up to 300 K, 10ps of equilibration, and 10ps of a production run. The last frame of the co-complex was considered as ligand pose with protein.

Statistical analysis

All the assays mentioned were performed in triplicates and expressed as Mean ± Standard Deviation (Mean ± SD). A p-value of $p<0.05$ was considered to be statistically significant. For qPCR, each reaction was performed in triplicates. Data were analyzed by one-way ANOVA followed by Tukey's multiple comparison test which was employed for the P-value determination using GraphPad Prism 6.0 (GraphPad Software, Inc., San Diego, CA). All bar and line plots were generated in GraphPad Prism.

Results

MA reduced cell growth and induced apoptosis in PC-3 cells via the intrinsic pathway

In an earlier report, we demonstrated that MA decreased the viability of PC3 cells [30]. In this study, we demonstrate that MA inhibited the growth rate of PC-3 cells in both a dose- and time-dependent manner (Figure 1a). At 200 µM, MA decreased mitochondrial membrane potential by 1.52-fold ($p<0.05$) after 24 h, indicative of apoptosis (Figure 1b). This observation was further corroborated by a significant upregulation in the mRNA expression levels of cytochrome c (43.4-fold; $p<0.001$), caspase 3 (18.7-fold; $p<0.001$), and caspase 9 (8.7-fold; $p<0.001$) (Figure 1c). These results suggested that MA induces apoptosis in PC-3 cells through an intrinsic, mitochondrial-dependent pathway.

MA reprograms lipid metabolism

To confirm the mechanism of action of MA in the regulation of lipid metabolism in PCa, the effect of MA was studied on the genes involved in lipogenesis (fatty acid and cholesterol synthesis), lipid transport, and lipid catabolism (lipolysis and fatty acid oxidation).

MA regulated key genes involved in fatty acid and cholesterol synthesis and their efflux

MA significantly decreased the mRNA expression of PPARγ by 5.2-fold ($p<0.001$) at 100 µM (Figure 2a). Additionally, MA reduced the mRNA levels of key fatty

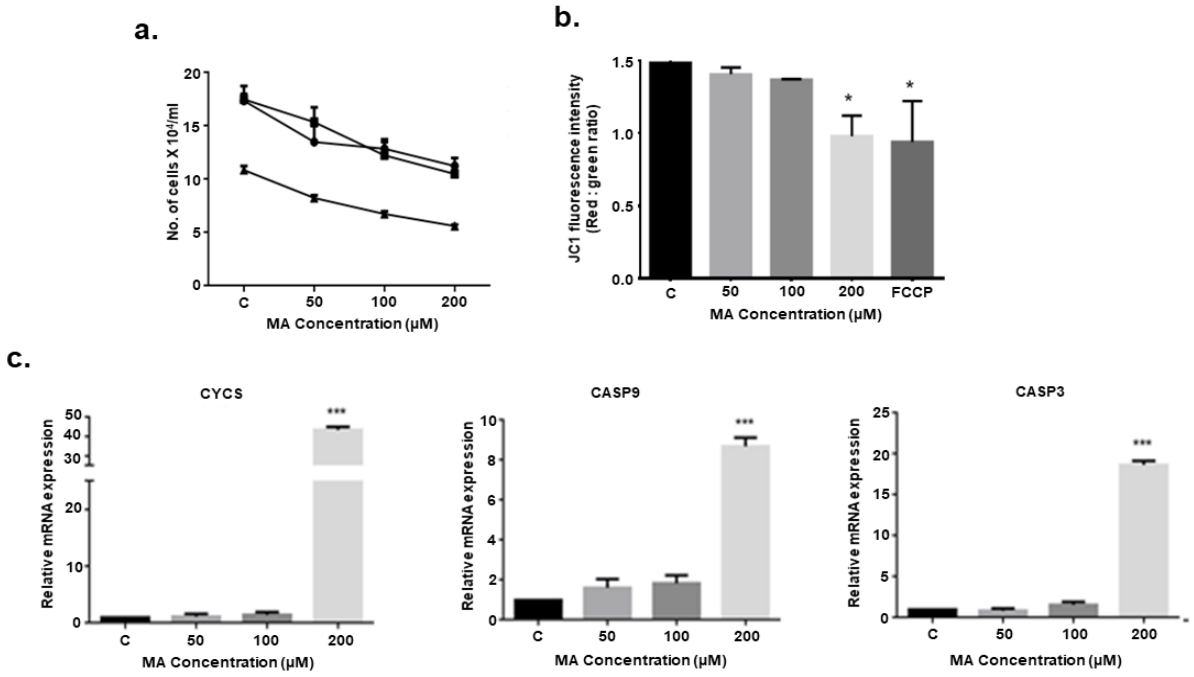

Figure 1. MA Decreased Cell Growth and Induced Apoptosis in PC3 Cells. After treatment of PC3 cells with MA, decrease in (a) Growth kinetics and (b) Mitochondrial membrane potential was observed. MA increased the mRNA expression of apoptosis-related genes (c) Cyt c, Caspase 9, and Caspase 3. Data has been represented as Mean ± standard deviation; n = 6. ***p < 0.001, **p < 0.01, *p < 0.05

acid biosynthesis genes: sterol regulatory element-binding protein 1 (SREBP1) by 3.1-fold ($p<0.01$), acetyl-CoA carboxylase (ACC) by 2.6-fold ($p<0.001$), ATP citrate lyase (ACLY) by 2-fold ($p<0.001$), fatty acid synthase (FASN) by 4.3-fold ($p<0.001$), and stearoyl CoA desaturase 1 (SCD1) by 2-fold ($p<0.05$) compared to untreated PC-3 cells. These findings were corroborated by a similar reduction in SREBP1 expression (3.7-fold; $p<0.001$) with Fatostatin (3 µM), a specific SREBP inhibitor. Furthermore, MA decreased the mRNA expression of cholesterol biosynthesis genes: sterol regulatory element-binding protein 2 (SREBP2) by 10.75-fold ($p<0.001$) and 3-hydroxy-3-methylglutaryl-CoA reductase (HMGCR) by 4.75-fold ($p<0.001$) at 100 µM (Figure 2b), with SREBP2 expression also reduced by 2.2-fold ($p<0.01$) upon Fatostatin treatment. Conversely, MA increased the mRNA levels of Liver X receptor (LxR) and ATP-binding cassette transporter (ABCA) by 1.5-fold and 1.2-fold ($p<0.05$), respectively (Figure 2c). Additionally, MA reduced intracellular lipid accumulation in the form of lipid droplets compared to untreated controls (Figure 2d).

MA regulates fatty acid elongation and lipid catabolism

At 100 µM, MA significantly decreased the mRNA levels of long-chain fatty acid synthesis genes, including ELOVL6 (7.3-fold; $p<0.001$), LIPE1 (1.6-fold; $p<0.01$), and ACSL1 (2.4-fold; $p>0.05$), compared to untreated cells (Figure 3a). Additionally, MA at the same concentration reduced the mRNA levels of genes involved in lipid utilization, such as CPT1A (6.2-fold; $p<0.001$) and SLC25A1 (2.6-fold; $p<0.001$) (Figure 3b). Thus, MA downregulated the key genes involved in lipid catabolism at mRNA levels.

In silico and in vitro validation revealed that MA regulates SHBG and DHRS4 expression

The data thus far indicate that MA regulates lipid metabolism by targeting pathways involved in fatty acid and cholesterol synthesis. To further elucidate the primary target of matairesinol, in silico and *in vitro* validation was performed.

SHBG and DHRS4 identified as a target for MA

SMILES format file of the ligand was uploaded to BindingDB [35] and PubChem [34] to identify the validated targets of MA, both the resources having curated experimental binding data of proteins and small molecules. PubChem showed MA to be active against SHBG with an IC_{50} of 0.3 µM for the displacement of 5 alpha-dihydrotestosterone and BindingDB showed SHBG as a target. Drugbank enlisted DHRS4 as a target for MA with unknown pharmacological action.

Matairesinol interacted with SHBG and DHRS4 proteins and reduced their mRNA expression

Molecular docking using AutoDock 4.2 was conducted to elucidate the binding interactions of matairesinol (MA) with sex hormone-binding globulin (SHBG). MA exhibited a docking score of -6.35 with SHBG. Detailed analysis of the interactions (Figure 4a and 4b) revealed that the carbonyl group of the butyrolactone moiety of MA interacts with the backbone NH of Met 107. Additionally, the two terminal benzene rings of MA form van der Waals (vDW) interactions with Phe 67, Val 105, Val 112, Ile 141, Leu 171, and Met 139. MA displayed a Tanimoto coefficient of 0.5 in comparison with estradiol, which co-crystallized with SHBG (PDB ID: 6PYF). While estradiol engaged in vDW interactions with Phe 67, Val

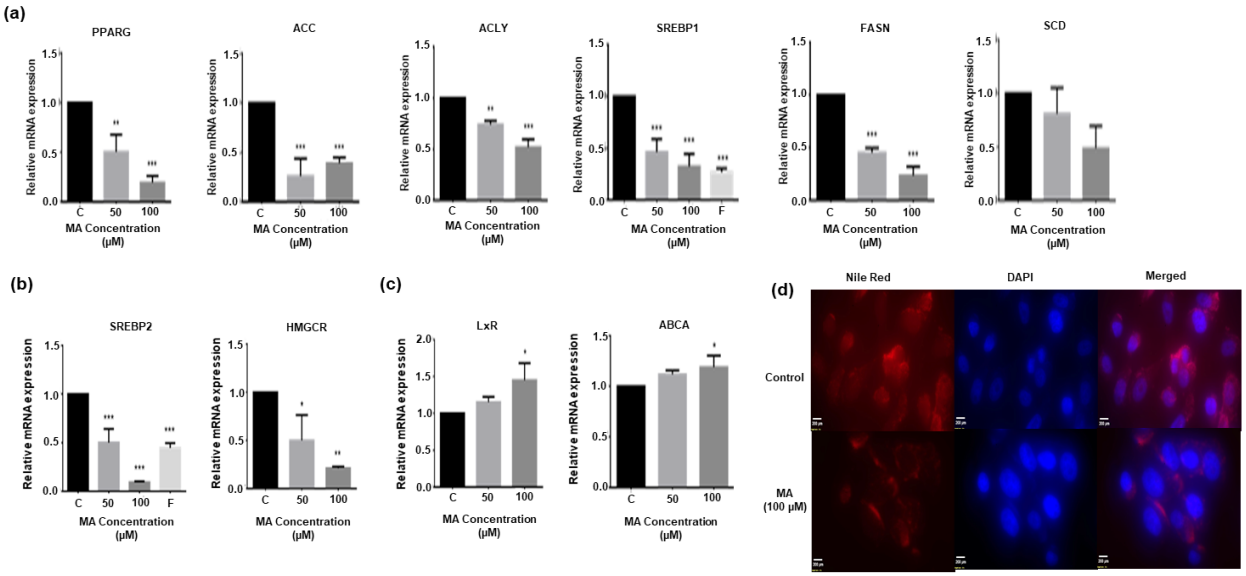

Figure 2. MA Regulated Key Genes Involved in Fatty Acid and Cholesterol Synthesis. MA reduced the mRNA expression of genes involved in (a) *de novo* fatty acid synthesis, (b) *de novo* cholesterol synthesis and (c) lipid transport. Transcript expression was measured in comparison to an untreated control, and β-actin was used as an internal control. F-Fatostatin. Each bar represents the mean ± standard deviation; n = 6. ***$p < 0.001$, **$p < 0.01$, *$p < 0.05$. Nile Red staining of lipid droplets showed that (d) MA reduced intracellular lipid accumulation in the cells. Representative images from one experiment have been shown

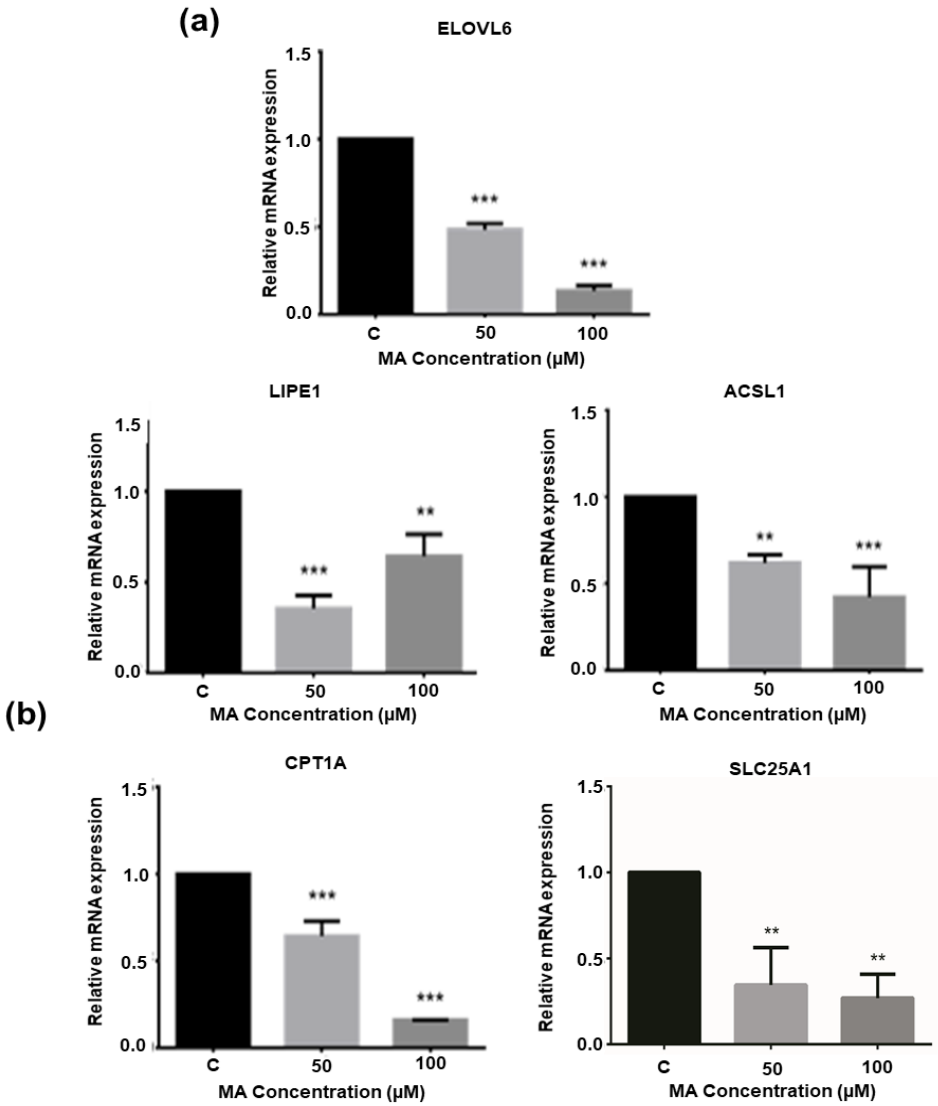

Figure 3. MA Regulated Fatty Acid Elongation and Lipid Catabolism. MA decreased mRNA expression of (a) lipolysis and (b) fatty acid oxidation genes. Relative mRNA expression was measured in comparison to an untreated control, and β-actin was used as an internal control. Each bar represents the mean ± standard deviation; n = 6. ***p < 0.001, **p < 0.01, *p < 0.05

105, Val 112, Ile 141, and Leu 171, the hydrogen bonding patterns differed due to variations in chemical groups.

For dehydrogenase/reductase member 4-like 2 (DHRS4), co-crystallized with MA (PDB ID: 2BGM), structural alignment with secoisolariciresinol dehydrogenase and subsequent refinement of the MA ligand placement through molecular dynamics revealed that the hydroxyl groups of MA's 2-methoxy phenol rings form hydrogen bonds with Pro 121, Ile 170, and Ser 174. The carbonyl group of the butyrolactone moiety interacts with Ser 176, while the aromatic rings engage in vDW interactions with Ile 170, Phe 179, Leu 214, Phe 219, and Leu 223. These interactions closely resemble those observed in the crystal structure of the plant protein. These docking results align with gene expression studies, which demonstrated that MA downregulates SHBG (1.32-fold; p<0.001) and DHRS4 (1.83-fold; p<0.001) expression (Figure 4e and 4f).

Discussion

Prostate cancer (PCa), a complex and multi-faceted disease, although having a good prognosis in the localized stage poses, significant challenges in treating its metastatic forms. In PCa, tumor cells undergo adaptions to survive in deficient levels of serum testosterone, known as the castration level in most patients, and eventually progress to develop mCRPC [53]. Stronger of AR signaling inhibition through APIs has led to enhance dedifferentiation of mCRPC into AR-negative disease, which is unresponsive to AR signaling inhibition and lacks a consensus on treatment [54, 55]. Thus, due to the scarcity of alternative therapies, the discovery of new druggable targets/pathways is urgently needed to improve clinical outcomes in PCa. To target AR-negative mCRPC, strategies may include either inducing AR re-expression (restoring chemosensitivity toward APIs) or directly targeting the AR-negative cells.

In AR negative PC3 cells, reduced fatty acid uptake through inhibition of CD36 decreased its proliferation,

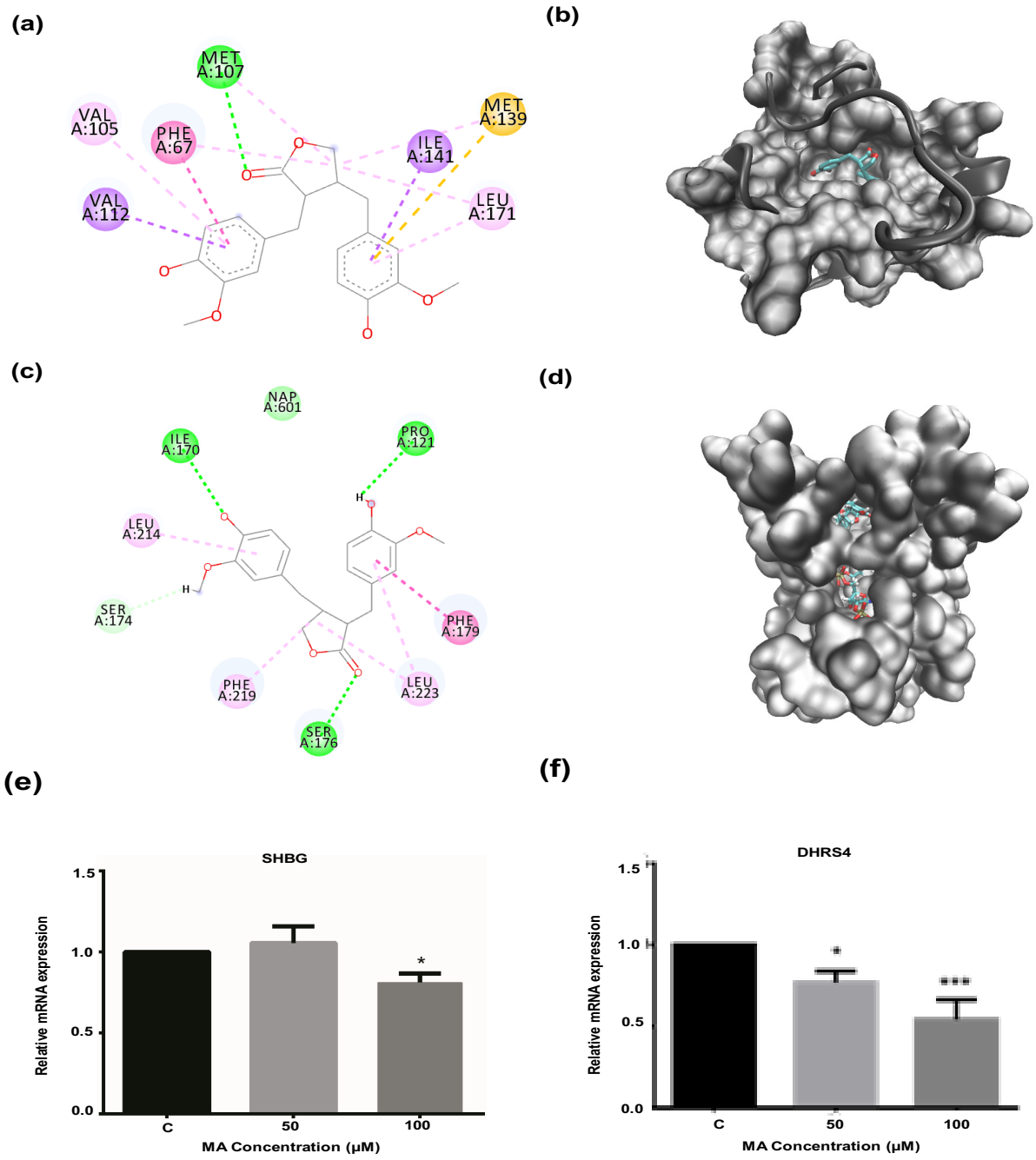

Figure 4. Matairesinol Interacted with SHBG and DHRS4 Proteins. The 2D and 3D binding interaction profile of MA with SHBG (a and b, respectively) and DHRS4 (c and d, respectively) has been shown. Correspondingly, MA reduced mRNA expression of SHBG (e) and DHRS4 (f). The dark green lines in panels a and c indicate hydrogen bonds; the light green indicates van der Waals interactions; the pink lines indicate alkyl and pi-alkyl interactions; and the yellow line indicates pi-sulfur interaction. mRNA expression was quantified relative to untreated control and β-actin was used as an internal control. Each bar represents the mean ± standard deviation; n = 6. ***$p < 0.001$, **$p < 0.01$, *$p < 0.05$

indicating that the lipid pathway plays an important role in its regulation [26]. Inhibition of *de novo* lipogenesis (by direct activation of AMPK) in PC3 (AR-negative mCRPC cell line) along with LNCaP (AR-positive mCRPC cell line) has been shown to induce mitotic arrest and apoptosis albeit to a lesser extent [56]. These studies indicate that even though AR-negative mCRPCs lack active AR function, they may still rely on *de novo* lipogenesis. Instead, they may utilize alternative pathways to sustain lipid metabolism and support tumor growth that need to be explored. In this line, various phytochemicals such as shown to induce anticancer activity in AR-negative PCa cell lines by targeting lipid metabolism. valproic acid [57], Celestrol [58], Citral [59], Tannic acid [60], Wogonin [61], Icaariin and Curcumol [62] have been.

In our earlier study, we have shown that MA reduced the viability of breast (MCF-7 and MDA-MB-231) and the prostate cancer cell lines (LNCaP and PC-3) with high selectivity relative to the normal cell lines [40, 36]. Recently, it was shown that MA exhibited anti-clonogenic and anti-migratory effects against PC3 [36]. Various lignans, including MA, have been reported to

downregulate anti-apoptotic proteins [63, 35, 64]. In the current study, we have observed a dose-dependent decrease in PC-3 cell growth at 24 h, 48 h, and 72 h. Further, MA treatment decreased the mitochondrial membrane potential of the cells and increased mRNA expression of cytochrome c, caspase 9, and caspase 3. Decrease in mitochondrial membrane potential triggers the release of cytochrome c from the mitochondria to the cytosol, leading to the activation of caspases and induction of apoptosis [65-67]. Thus, this indicated that MA induced apoptosis in PC-3 cells through activation of cytochrome C and caspases.

Truncation of the tricarboxylic acid (TCA) cycle in the normal prostate epithelial cells leads to zinc accumulation through inhibition of enzyme m-aconitase, which converts citrate to isocitrate [23]. However, reactivation of the TCA cycle in PCa cells leads to oxidation of citrate which further gets converted to acetyl CoA for *de novo* lipid synthesis. Thus, PCa cells display lipogenic phenotype and enhanced lipid metabolism than the normal cells [23]. The *in vitro* models of PCa cell lines, including PC3 consistently show higher lipid levels compared to the non-neoplastic prostate cells [68]. In the present study, It was observed that MA treatment altered the mRNA levels of the genes involved in the lipid metabolism pathway. Inhibition of *de novo* fatty acid and cholesterol synthesis, after MA treatment, is evident by downregulation of mRNA levels of PPARγ, SREBP-1, ACC, ACLY, FASN, SREBP2, and HMGCR. PPARγ plays an oncogenic role in the development and progression of PCa and presents an increased severity of castration resistance [25]. In patients with low PTEN expression, PPARγ is correlated with prostate cancer grade and associated with worse disease-specific survival, while PPARγ inhibition suppressed tumor growth *in vivo* by downregulating lipid synthesis [69]. SREBPs regulate *de novo* fatty acid and cholesterol biosynthesis through interaction with cis-acting Sterol Regulatory Element (SRE) present in the promoter regions of genes associated with these pathways [70]. SREBP-1 is associated with the activation of genes involved in *de novo* fatty acid synthesis, including ACC, ACLY, and FASN. A study has shown that mCRPC tumors identified SREBPs as crucial targets, with their inhibition shown to be significantly effective in the PC3 cell model [24]. These findings imply that MA might have inhibited the growth of the PC3 cell line by reducing intracellular fatty acid levels.

Assessment of databases such as Oncomine and cBIOPORTAL has revealed the upregulation of several genes associated with fatty acid synthesis (ACC, ACLY, and FASN), fatty acid desaturation (SCD1), a long chain fatty acyl-CoA synthetases- ACSL-1, ACSL-3, ACSL-5), fatty acid elongation (ELOVL5, 6, 7), fatty acid oxidation (CPT1 and ECl2), and cholesterol synthesis (HMGCR) in PCa especially metastatic disease as compared to normal epithelial tissue [71]. Various enzymes involved in fatty acid production have been linked to the development of PCa [72]. Inhibiting ACLY in PCa cells activates AMPK, which suppresses AR levels and inhibits cell proliferation, revealing a feedback loop among AMPK, ACLY, and AR [73]. ACC1 and FASN are reported to be overexpressed in prostatic intraepithelial neoplasia (early-stage) and PCa (advanced-stage) [74]. SCD is involved in the desaturation of saturated fatty acids (SFAs) to Δ9-monounsaturated fatty acids (MUFAs)- stearic (18:0) and palmitic acid (16:0) to oleic (18:1) and palmitoleic acid (16:1). These SFA and MUFA are basic components of cell membrane and serve as energy and signaling molecules. SCD1 expression is found to be associated with the activation of cancer-stem cells (CSCs) markers such as ALDH1A1, Oct4, and Nanog via regulation of Hippo signaling and the Wnt-β-catenin signaling pathways [75]. Overall, SCD has been shown to increase ferroptosis and apoptosis while inhibiting cancer cell proliferation, migration, and invasion [76].

SREBP-2 regulates HMGCR, a rate-limiting enzyme and cholesterogenesis checkpoint, to mediate cholesterol biosynthesis. Cholesterol levels are controlled within the cell through uptake, synthesis, and efflux [77]. MA treatment resulted in a significant increase in LXR mRNA levels with SREBP2 downregulation. The expression of the ABCA1 and ABCG1- LXR downstream genes implicated in cholesterol efflux [78] was also significantly increased post-MA treatment. PCa cells exhibited increased SREBP-2 activity while decreasing LXR activity, resulting into higher cholesterol levels. LXR heterodimerizes with the retinoid X receptor (RXR) and prevents cholesterol accumulation [79]. These findings imply that MA inhibited the growth of the PC-3 cell line by reducing intracellular cholesterol levels.

In comparison to the normal adult mammalian tissues, cancer cells have a higher number of lipid droplets (LDs) due to increased lipid uptake and *de novo* lipogenesis [80]. LDs are cellular organelles composed of neutral fatty acids and cholesterol esters [80-82]. LDs are central to cellular lipid and energy homeostasis and support cancer cell proliferation, migration, and survival by mitigating cellular stress and supplying substrates for membrane lipid synthesis and β-oxidation [83, 84]. In this study, we found that MA reduced the intracellular lipid accumulation in PC3 cells. Generally, cancer cells lacking LDs are more prone to apoptosis [80]. One of the studies reported an accumulation of cholesteryl esters in human tissues displaying high-grade and metastatic PCa [85], whereas their reduction in PCa (especially in PC3 cell line) inhibited cell proliferation, apoptosis, and migration [86]. The reduction in lipid droplet accumulation in MA-treated PC3 cells may have contributed to the inhibition of proliferation and induction of apoptosis, warranting further specific investigation.

In addition to lipogenesis, lipolysis, and lipid oxidation have also been shown to be elevated in various human cancers [87]. Lipolysis is a process involving the breakdown of triglycerides stored in the lipid droplets to free fatty acids. Lipid oxidation is the metabolic process in which free fatty acids are broken down to generate energy in the form of ATP. In this study, MA was found to downregulate the mRNA levels of the key genes involved in fatty acid oxidation (CPT, SLC25A1), fatty acid elongation and lipolysis (ELOVL6, LIPE, ACSL1). In mCRPC, the expression of ACSL and CPT1 is increased, and inhibition of ACSL1 has been shown

to decrease lipid droplet accumulation, mitochondrial respiration, β-oxidation, and ATP production by regulating CPT1 activity [89-90]. CPT1A amplification in mCRPC, leads to excess acetyl-CoA production, driving histone acetylation, tumor growth, and therapy resistance [91]. MA downregulated CPT1A and ACSL1 mRNA expression, potentially reducing PCa cell growth and resensitizing them to therapy. ELOVL6 is a long-chain fatty-Acyl elongase. Enhanced ELOVL6 expression is reported to be associated with tumor progression [92]. Lipase E (LIPE), also termed hormone-sensitive lipase (HSL), is involved in the release of free fatty acids from diacylglycerol and long-chain fatty acyl-CoA synthetases [93]. SLC25A1 helps maintain cytoplasmic citrate levels, which positively modulate ACC, a key enzyme in fatty acid synthesis, and is upregulated in various cancers to promote tumor growth [94]. Downregulation of CPT1A and SLC25A1 by MA could result in a low citrate concentration, thereby affecting the lipid metabolism pathway. The overall data suggested that MA exhibited therapeutic potential to modulate the lipid oxidation process, which serves as an important part of cancer metabolic reprogramming and is yet to be fully explored in PCa therapeutics.

Target identification using BindingDB, PubChem, and DrugBank suggested SHBG and DHRS4L2 as validated targets of MA, based on the experimental data deposited in these databases. This was further validated by *in vitro* studies, displaying downregulation of mRNA expression of SHBG and DHRS4 in PC3 cell line post-MA treatment. SHBG is a 90 KD glycoprotein, a nuclear hormone receptor superfamily member. It binds to sex hormones testosterone and estradiol, with a higher affinity for 5 alpha-dihydrotestosterone (DHT), and plays a role in the transport of DHT inside prostate cells, which act as a precursor for PCa. It further stimulates the expression of AR-regulated genes associated with *de novo* lipogenesis pathway such as PPARγ and its downstream transcription factors, SREBP1 and SREBP2 [95, 51]. DHRS4 is an oxidoreductase enzyme that is involved in retinol metabolism and fatty acid breakdown. It converts 9-cis retinol to metabolically active form, All cis-retinol, which is a ligand for LxR/RxR receptors that activates downstream PPARγ signaling pathway [96]. Our computational studies revealed that MA is bound to the active site of both SHBG and DHRS4, the latter being structurally similar to the plant protein, secoisolariciresinol dehydrogenase. Both the proteins belong to the Plant short-chain dehydrogenase (SDR) superfamily and have an α/β domain structure, including the dinucleotide-binding Rossmann fold. Thus, this binding MA to SHBG and DHRS4 resulted into downregulates the *de novo* lipogenesis pathway that fatty acid and cholesterol synthesis, thereby downmodulating downstream effectors of PPARγ signaling (Scheme 1). This resulted in decreased mRNA expression of genes involved in lipid reprogramming, ultimately inducing apoptosis through mitochondrial membrane depolarization, characterized by the release of caspase 3 and 9. Thus, MA could potentiate the regulation of lipid metabolism, which could in effect halt prostate cancer progression.

Metabolic reprogramming is one of the hallmarks of the malignant phenotype in cancer. In PCa, *de novo*

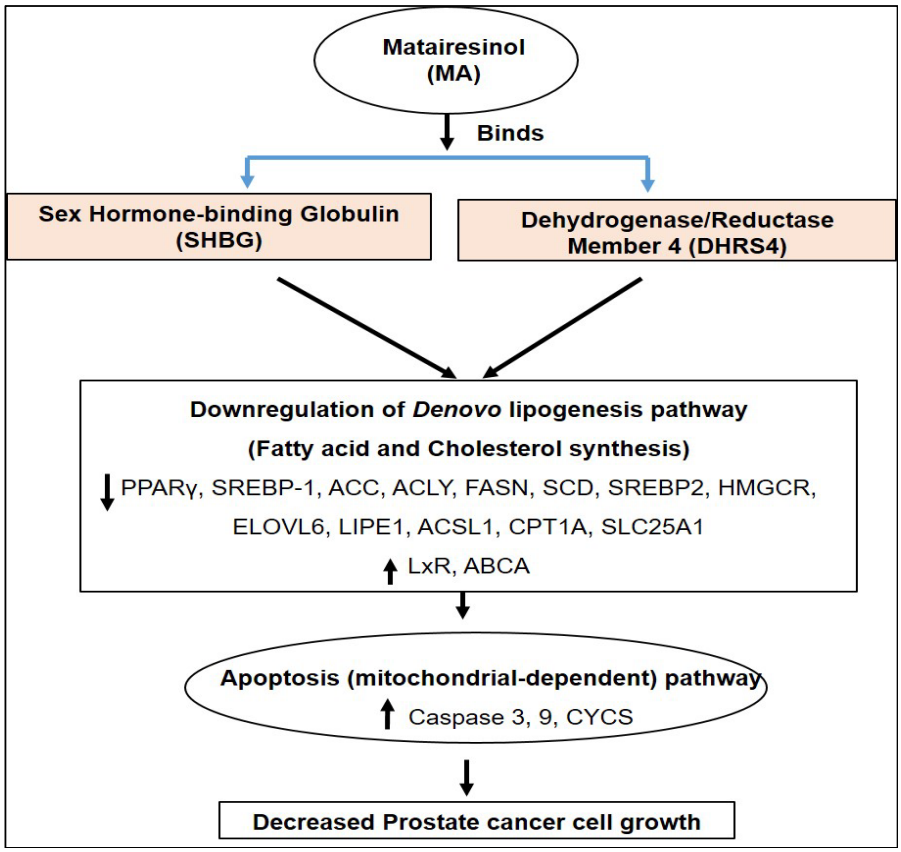

Scheme 1. Schematic Representation of Matairesinol-Induced Apoptosis via Lipid Metabolism Reprogramming in AR-Independent Prostate Cancer Cells- PC3

fatty acid synthesis pathway plays a key role in cell membrane biosynthesis, allowing rapid proliferation, providing energy during metabolic stress conditions, and inhibiting apoptosis. Alternatively, *de novo* cholesterol synthesis is associated with internal androgen production to sustain activation of signaling pathways that promote invasion and metastasis of PCa cells. The present report has elucidated the potential of the plant lignan, MA, rewiring the lipid metabolism reprogramming in PCa cells through suppression of *de novo* lipogenesis pathway, which includes fatty acid and cholesterol synthesis, fatty acid oxidation, lipolysis, decrease in lipid accumulation in lipid droplets and induction of apoptosis through the intrinsic pathway. However, further detailed studies are warranted to confirm the mechanistic endpoints of MA, to promote it as a potential drug candidate against lipid reprogramming in prostate cancer.

Author Contribution Statement

Minal Mahajan: Investigation, Methodology, Formal analysis, Writing - original draft; Gauri Ghodke: Investigation, Methodology, Formal analysis; Manali Joshi: Investigation, Methodology, Formal analysis, Writing -review & editing; Amol Chaudhary: Writing -Review, editing; Ruchika Kaul-Ghanekar: Conceptualization, Resources, Supervision, Methodology, Formal analysis, Writing - original draft, review & editing.

Acknowledgements

We thank IRSHA, Bharati Vidyapeeth (Deemed to be) University for supporting this work.

Scientific Approval / Thesis Information

This study is a part of an approved thesis of Ms. Minal Mahajan, a PhD student under the Ph.D. program in Biotechnology at Bharati Vidyapeeth (Deemed to be University), Pune. It has been reviewed and approved by the institutional research committee.

Ethical Approval

This study used an established human prostate cancer cell line and did not involve human participants or animal subjects. Therefore, ethical approval was not required. However, all experimental procedures complied with institutional biosafety and research guidelines of Bharati Vidyapeeth (Deemed to be University), Pune.

Conflict of Interest

The authors declare that there are no conflicts of interest.

References

1. WHO. Global cancer observatory [database on the Internet]. 2022. Available from: https://gco.iarc.fr/en.
2. James ND, Tannock I, N'Dow J, Feng F, Gillessen S, Ali SA, et al. The lancet commission on prostate cancer: Planning for the surge in cases. Lancet. 2024;403(10437):1683-722. https://doi.org/10.1016/S0140-6736(24)00651-2.
3. Sung H, Ferlay J, Siegel RL, Laversanne M, Soerjomataram I, Jemal A, et al. Global cancer statistics 2020: Globocan estimates of incidence and mortality worldwide for 36 cancers in 185 countries. CA Cancer J Clin. 2021;71(3):209-49. https://doi.org/10.3322/caac.21660.
4. Mathur P, Sathishkumar K, Chaturvedi M, Das P, Sudarshan KL, Santhappan S, et al. Cancer statistics, 2020: Report from national cancer registry programme, india. JCO Glob Oncol. 2020(6):1063-75. https://doi.org/10.1200/go.20.00122.
5. Kumar A, Yadav S, Krishnappa RS, Gautam G, Raghavan N, Bakshi G, et al. The urological society of india guidelines for the evaluation and management of prostate cancer (executive summary). Indian J Urol. 2022;38(4):252-7. https://doi.org/10.4103/iju.iju_232_22.
6. Hebert JR, Ghumare SS, Gupta PC. Stage at diagnosis and relative differences in breast and prostate cancer incidence in india-comparison with the united states. Asian Pac J Cancer Prev. 2006;7(4):547-55.
7. Tewari AK, Srivastava A, Sooriakumaran P, Grover S, Desir S, Dev H, et al. Pathological outcomes and strategies to achieve optimal cancer control during robotic radical prostatectomy in asian-indian men. Indian J Urol. 2011;27(3):326-30. https://doi.org/10.4103/0970-1591.85428.
8. Schaeffer EM, Srinivas S, Adra N, An Y, Barocas D, Bitting R, et al. Prostate cancer, version 4.2023, nccn clinical practice guidelines in oncology. J Natl Compr Canc Netw. 2023;21(10):1067-96. https://doi.org/10.6004/jnccn.2023.0050.
9. Sandhu S, Moore CM, Chiong E, Beltran H, Bristow RG, Williams SG. Prostate cancer. Lancet. 2021;398(10305):1075-90. https://doi.org/10.1016/S0140-6736(21)00950-8.
10. Miller DR, Ingersoll MA, Teply BA, Lin M-F. Targeting treatment options for castration-resistant prostate cancer. Am J Clin Exp Urol. 2021;9(1):101-20.
11. Maluf FC, Pereira FMT, Silva AG, Dettino ALA, Cardoso APG, Sasse AS, et al. Consensus on the treatment and follow-up for metastatic castration-resistant prostate cancer: A report from the first global prostate cancer consensus conference for developing countries (pcccdc). JCO Glob Oncol. 2021(7):559-71. https://doi.org/10.1200/go.20.00511.
12. Patrikidou A, Loriot Y, Eymard JC, Albiges L, Massard C, Ileana E, et al. Who dies from prostate cancer? Prostate Cancer Prostatic Dis. 2014;17(4):348-52. https://doi.org/10.1038/pcan.2014.35.
13. Omlin A, Pezaro C, Mukherji D, Mulick Cassidy A, Sandhu S, Bianchini D, et al. Improved survival in a cohort of trial participants with metastatic castration-resistant prostate cancer demonstrates the need for updated prognostic nomograms. Eur Urol. 2013;64(2):300-6. https://doi.org/10.1016/j.eururo.2012.12.029.
14. Ahmad F, Cherukuri MK, Choyke PL. Metabolic reprogramming in prostate cancer. Br J Cancer. 2021;125(9):1185-96. https://doi.org/10.1038/s41416-021-01435-5.
15. Bristow RG, Berlin A, Dal Pra A. An arranged marriage for precision medicine: Hypoxia and genomic assays in localized prostate cancer radiotherapy. Br J Radiol. 2014;87(1035):20130753. https://doi.org/10.1259/bjr.20130753.
16. Hanahan D. Hallmarks of cancer: New dimensions. Cancer Discov. 2022;12(1):31-46. https://doi.org/10.1158/2159-8290.CD-21-1059.
17. Yoshida GJ. Metabolic reprogramming: The emerging concept and associated therapeutic strategies. J Exp Clin Cancer Res. 2015;34:111. https://doi.org/10.1186/s13046-015-0221-y.
18. Cheng C, Geng F, Cheng X, Guo D. Lipid metabolism

reprogramming and its potential targets in cancer. Cancer Commun (Lond). 2018;38(1):27. https://doi.org/10.1186/s40880-018-0301-4.
19. Mak B, Lin HM, Kwan EM, Fettke H, Tran B, Davis ID, et al. Combined impact of lipidomic and genetic aberrations on clinical outcomes in metastatic castration-resistant prostate cancer. BMC Med. 2022;20(1):112. https://doi.org/10.1186/s12916-022-02298-0.
20. Petrella G, Corsi F, Ciufolini G, Germini S, Capradossi F, Pelliccia A, et al. Metabolic reprogramming of castration-resistant prostate cancer cells as a response to chemotherapy. Metabolites. 2022;13(1). https://doi.org/10.3390/metabo13010065.
21. Sena LA, Denmeade SR. Fatty acid synthesis in prostate cancer: Vulnerability or epiphenomenon? Cancer Res. 2021;81(17):4385-93. https://doi.org/10.1158/0008-5472.CAN-21-1392.
22. Liu S, Lai J, Feng Y, Zhuo Y, Zhang H, Chen Y, et al. Acetyl-coa carboxylase 1 depletion suppresses *de novo* fatty acid synthesis and mitochondrial beta-oxidation in castration-resistant prostate cancer cells. J Biol Chem. 2023;299(1):102720. https://doi.org/10.1016/j.jbc.2022.102720.
23. Mah CY, Nassar ZD, Swinnen JV, Butler LM. Lipogenic effects of androgen signaling in normal and malignant prostate. Asian J Urol. 2020;7(3):258-70. https://doi.org/10.1016/j.ajur.2019.12.003.
24. Wei G, Zhu H, Zhou Y, Pan Y, Yi B, Bai Y. Single-cell sequencing revealed metabolic reprogramming and its transcription factor regulatory network in prostate cancer. Transl Oncol. 2024;44:101925. https://doi.org/10.1016/j.tranon.2024.101925.
25. Hartley A, Ahmad I. The role of ppargamma in prostate cancer development and progression. Br J Cancer. 2023;128(6):940-5. https://doi.org/10.1038/s41416-022-02096-8.
26. Watt MJ, Clark AK, Selth LA, Haynes VR, Lister N, Rebello R, et al. Suppressing fatty acid uptake has therapeutic effects in preclinical models of prostate cancer. Sci Transl Med. 2019;11(478). https://doi.org/10.1126/scitranslmed.aau5758
27. Elix CC, Salgia MM, Otto-Duessel M, Copeland BT, Yoo C, Lee M, et al. Peroxisome proliferator-activated receptor gamma controls prostate cancer cell growth through ar-dependent and independent mechanisms. Prostate. 2020;80(2):162-72. https://doi.org/10.1002/pros.23928.
28. McGarry JD, Takabayashi Y, Foster DW. The role of malonyl-coa in the coordination of fatty acid synthesis and oxidation in isolated rat hepatocytes. J Biol Chem. 1978;253(22):8294-300. https://doi.org/10.1016/s0021-9258(17)34395-8.
29. Bastos DC, Ribeiro CF, Ahearn T, Nascimento J, Pakula H, Clohessy J, et al. Genetic ablation of fasn attenuates the invasive potential of prostate cancer driven by pten loss. J Pathol. 2021;253(3):292-303. https://doi.org/10.1002/path.5587.
30. Mukhija M, Joshi BC, Bairy PS, Bhargava A, Sah AN. Lignans: A versatile source of anticancer drugs. Beni Suef Univ J Basic Appl Sci. 2022;11(1):76. https://doi.org/10.1186/s43088-022-00256-6.
31. Su S, Cheng X, Wink M. Cytotoxicity of arctigenin and matairesinol against the t-cell lymphoma cell line ccrf-cem. J Pharm Pharmacol. 2015;67(9):1316-23. https://doi.org/10.1111/jphp.12426.
32. Abarzua S, Serikawa T, Szewczyk M, Richter D-U, Piechulla B, Briese V. Antiproliferative activity of lignans against the breast carcinoma cell lines mcf 7 and bt 20. Arch Gynecol Obstet. 2012;285(4):1145-51. https://doi.org/10.1007/s00404-011-2120-6.
33. Zhu Y, Kawaguchi K, Kiyama R. Differential and directional estrogenic signaling pathways induced by enterolignans and their precursors. PLoS One. 2017;12(2):e0171390. https://doi.org/10.1371/journal.pone.0171390.
34. Lee W, Song G, Bae H. Matairesinol induces mitochondrial dysfunction and exerts synergistic anticancer effects with 5-fluorouracil in pancreatic cancer cells. Mar Drugs. 2022;20(8). https://doi.org/10.3390/md20080473.
35. Peuhu E, Rivero-Muller A, Stykki H, Torvaldson E, Holmbom T, Eklund P, et al. Inhibition of akt signaling by the lignan matairesinol sensitizes prostate cancer cells to trail-induced apoptosis. Oncogene. 2010;29(6):898-908. https://doi.org/10.1038/onc.2009.386.
36. Rajadnya R, Sharma N, Mahajan A, Ulhe A, Patil R, Hegde M, et al. Novel systems biology experimental pipeline reveals matairesinol's antimetastatic potential in prostate cancer: An integrated approach of network pharmacology, bioinformatics, and experimental validation. Brief Bioinform. 2024;25(5). https://doi.org/10.1093/bib/bbae466.
37. Xu P, Huang MW, Xiao CX, Long F, Wang Y, Liu SY, et al. Matairesinol suppresses neuroinflammation and migration associated with src and erk1/2-nf-kappab pathway in activating bv2 microglia. Neurochem Res. 2017;42(10):2850-60. https://doi.org/10.1007/s11064-017-2301-1.
38. Yamawaki M, Nishi K, Nishimoto S, Yamauchi S, Akiyama K, Kishida T, et al. Immunomodulatory effect of (--)-matairesinol in vivo and ex vivo. Biosci Biotechnol Biochem. 2011;75(5):859-63. https://doi.org/10.1271/bbb.100781.
39. Lee B, Kim KH, Jung HJ, Kwon HJ. Matairesinol inhibits angiogenesis via suppression of mitochondrial reactive oxygen species. Biochem Biophys Res Commun. 2012;421(1):76-80. https://doi.org/10.1016/j.bbrc.2012.03.114.
40. Mahajan M, Suryavanshi S, Bhowmick S, Alasmary FA, Almutairi TM, Islam MA, et al. Matairesinol, an active constituent of hc9 polyherbal formulation, exhibits hdac8 inhibitory and anticancer activity. Biophys Chem. 2021;273:106588. https://doi.org/10.1016/j.bpc.2021.106588.
41. Wu S, Wang J, Fu Z, Familiari G, Relucenti M, Aschner M, et al. Matairesinol nanoparticles restore chemosensitivity and suppress colorectal cancer progression in preclinical models: Role of lipid metabolism reprogramming. Nano Lett. 2023;23(5):1970-80. https://doi.org/10.1021/acs.nanolett.3c00035.
42. Kaighn ME, Narayan KS, Ohnuki Y, Lechner JF, Jones LW. Establishment and characterization of a human prostatic carcinoma cell line (pc-3). Invest urol. 1979;17(1):16-23.
43. Cheng S, Yu X. The spectrum of neuroendocrine differentiation in prostate cancer. Prostate Cancer Prostatic Dis. 2021;24(4):1214-5. https://doi.org/10.1038/s41391-021-00386-5.
44. Deshpande R, Mansara P, Suryavanshi S, Kaul-Ghanekar R. Alpha-linolenic acid regulates the growth of breast and cervical cancer cell lines through regulation of no release and induction of lipid peroxidation. J Mol Biochem. 2013;2:6-17.
45. Aphale S, Shinde K, Pandita S, Mahajan M, Raina P, Mishra JN, et al. Panchvalkala, a traditional ayurvedic formulation, exhibits antineoplastic and immunomodulatory activity in cervical cancer cells and c57bl/6 mouse papilloma model. J Ethnopharmacol. 2021;280:114405. https://doi.org/10.1016/j.jep.2021.114405.
46. Schmittgen TD, Livak KJ. Analyzing real-time pcr data by the comparative c(t) method. Nat Protoc. 2008;3(6):1101-8. https://doi.org/10.1038/nprot.2008.73.
47. Gilson MK, Liu T, Baitaluk M, Nicola G, Hwang L,

Chong J. Bindingdb in 2015: A public database for medicinal chemistry, computational chemistry and systems pharmacology. Nucleic Acids Res. 2016;44(D1):D1045-53. https://doi.org/10.1093/nar/gkv1072.
48. Kim S. Exploring chemical information in pubchem. Curr Protoc. 2021;1(8):e217. https://doi.org/10.1002/cpz1.217.
49. Wishart DS, Feunang YD, Guo AC, Lo EJ, Marcu A, Grant JR, et al. Drugbank 5.0: A major update to the drugbank database for 2018. Nucleic Acids Res. 2018;46(D1):D1074-D82. https://doi.org/10.1093/nar/gkx1037.
50. Morris GM, Huey R, Lindstrom W, Sanner MF, Belew RK, Goodsell DS, et al. Autodock4 and autodocktools4: Automated docking with selective receptor flexibility. J Comput Chem. 2009;30(16):2785-91. https://doi.org/10.1002/jcc.21256.
51. Round P, Das S, Wu TS, Wahala K, Van Petegem F, Hammond GL. Molecular interactions between sex hormone-binding globulin and nonsteroidal ligands that enhance androgen activity. J Biol Chem. 2020;295(5):1202-11. https://doi.org/10.1074/jbc.RA119.011051.
52. Youn B, Moinuddin SG, Davin LB, Lewis NG, Kang C. Crystal structures of apo-form and binary/ternary complexes of podophyllum secoisolariciresinol dehydrogenase, an enzyme involved in formation of health-protecting and plant defense lignans. J Biol Chem. 2005;280(13):12917-26. https://doi.org/10.1074/jbc.M413266200.
53. Hoang DT, Iczkowski KA, Kilari D, See W, Nevalainen MT. Androgen receptor-dependent and -independent mechanisms driving prostate cancer progression: Opportunities for therapeutic targeting from multiple angles. Oncotarget. 2017;8(2):3724-45. https://doi.org/10.18632/oncotarget.12554.
54. Formaggio N, Rubin MA, Theurillat JP. Loss and revival of androgen receptor signaling in advanced prostate cancer. Oncogene. 2021;40(7):1205-16. https://doi.org/10.1038/s41388-020-01598-0.
55. Bluemn EG, Coleman IM, Lucas JM, Coleman RT, Hernandez-Lopez S, Tharakan R, et al. Androgen receptor pathway-independent prostate cancer is sustained through fgf signaling. Cancer Cell. 2017;32(4):474-89 e6. https://doi.org/10.1016/j.ccell.2017.09.003.
56. Zadra G, Photopoulos C, Tyekucheva S, Heidari P, Weng QP, Fedele G, et al. A novel direct activator of ampk inhibits prostate cancer growth by blocking lipogenesis. EMBO Mol Med. 2014;6(4):519-38. https://doi.org/10.1002/emmm.201302734.
57. Pang B, Zhang J, Zhang X, Yuan J, Shi Y, Qiao L. Inhibition of lipogenesis and induction of apoptosis by valproic acid in prostate cancer cells via the c/ebpalpha/srebp-1 pathway. Acta Biochim Biophys Sin (Shanghai). 2021;53(3):354-64. https://doi.org/10.1093/abbs/gmab002.
58. Arisan ED, Rencuzogullari O, Coban M, Sevgin B, Obakan-Yerlikaya P, Çoker-Gürkan A, et al. The role of the pi3k/akt/mtor signaling axis in the decision of the celastrol-induced cell death mechanism related to the lipid regulatory pathway in prostate cancer cells. Phytochem Lett. 2020;39:73-83. https://doi.org/10.1016/j.phytol.2020.06.007.
59. Balusamy SR, Perumalsamy H, Veerappan K, Huq MA, Rajeshkumar S, Lakshmi T, et al. Citral induced apoptosis through modulation of key genes involved in fatty acid biosynthesis in human prostate cancer cells: In silico and in vitro study. Biomed Res Int. 2020;2020:6040727. https://doi.org/10.1155/2020/6040727.
60. Nagesh PKB, Chowdhury P, Hatami E, Jain S, Dan N, Kashyap VK, et al. Tannic acid inhibits lipid metabolism and induce ros in prostate cancer cells. Sci Rep. 2020;10(1):980. https://doi.org/10.1038/s41598-020-57932-9.
61. Sun Y, Guo W, Guo Y, Lin Z, Wang D, Guo Q, et al. Apoptosis induction in human prostate cancer cells related to the fatty acid metabolism by wogonin-mediated regulation of the akt-srebp1-fasn signaling network. Food Chem Toxicol. 2022;169:113450. https://doi.org/10.1016/j.fct.2022.113450.
62. Xu W, Ding J, Li B, Sun T, You X, He Q, et al. Effects of icariin and curcumol on autophagy, ferroptosis, and lipid metabolism based on mir-7/m-tor/srebp1 pathway on prostate cancer. Biofactors. 2023;49(2):438-56. https://doi.org/10.1002/biof.1927.
63. Peuhu E, Paul P, Remes M, Holmbom T, Eklund P, Sjoholm R, et al. The antitumor lignan nortrachelogenin sensitizes prostate cancer cells to trail-induced cell death by inhibition of the akt pathway and growth factor signaling. Biochem Pharmacol. 2013;86(5):571-83. https://doi.org/10.1016/j.bcp.2013.05.026.
64. Yatkin E, Polari L, Laajala TD, Smeds A, Eckerman C, Holmbom B, et al. Novel lignan and stilbenoid mixture shows anticarcinogenic efficacy in preclinical pc-3m-luc2 prostate cancer model. PLoS One. 2014;9(4):e93764. https://doi.org/10.1371/journal.pone.0093764.
65. Glover HL, Schreiner A, Dewson G, Tait SWG. Mitochondria and cell death. Nature Cell Biology. 2024. https://doi.org/10.1038/s41556-024-01429-4.
66. Bock FJ, Tait SWG. Mitochondria as multifaceted regulators of cell death. Nat Rev Mol Cell Biol. 2020;21(2):85-100. https://doi.org/10.1038/s41580-019-0173-8.
67. Lartigue L, Kushnareva Y, Seong Y, Lin H, Faustin B, Newmeyer DD. Caspase-independent mitochondrial cell death results from loss of respiration, not cytotoxic protein release. Mol Biol Cell. 2009;20(23):4871-84. https://doi.org/10.1091/mbc.e09-07-0649.
68. Nambiar DK, Deep G, Singh RP, Agarwal C, Agarwal R. Silibinin inhibits aberrant lipid metabolism, proliferation and emergence of androgen-independence in prostate cancer cells via primarily targeting the sterol response element binding protein 1. Oncotarget. 2014;5(20). https://doi.org/10.18632/oncotarget.2488.
69. Ahmad I, Mui E, Galbraith L, Patel R, Tan EH, Salji M, et al. Sleeping beauty screen reveals pparg activation in metastatic prostate cancer. Proc Natl Acad Sci U S A. 2016;113(29):8290-5. https://doi.org/10.1073/pnas.1601571113.
70. Zhao Q, Lin X, Wang G. Targeting srebp-1-mediated lipogenesis as potential strategies for cancer. Front Oncol. 2022;12:952371. https://doi.org/10.3389/fonc.2022.952371.
71. Eidelman E, Twum-Ampofo J, Ansari J, Siddiqui MM. The metabolic phenotype of prostate cancer. Front Oncol. 2017;7:131. https://doi.org/10.3389/fonc.2017.00131.
72. Scheinberg T, Mak B, Butler L, Selth L, Horvath LG. Targeting lipid metabolism in metastatic prostate cancer. Ther Adv Med Oncol. 2023;15:17588359231152839. https://doi.org/10.1177/17588359231152839.
73. Shah S, Carriveau WJ, Li J, Campbell SL, Kopinski PK, Lim H-W, et al. Targeting acly sensitizes castration-resistant prostate cancer cells to ar antagonism by impinging on an acly-ampk-ar feedback mechanism. Oncotarget. 2016;7(28):43713-30. https://doi.org/10.18632/oncotarget.9666.
74. Kim SH, Singh KB, Hahm ER, Lokeshwar BL, Singh SV. Withania somnifera root extract inhibits fatty acid synthesis in prostate cancer cells. J Tradit Complement Med. 2020;10(3):188-97. https://doi.org/10.1016/j.jtcme.2020.02.002.
75. Min JY, Kim DH. Stearoyl-coa desaturase 1 as a therapeutic biomarker: Focusing on cancer stem cells. Int J Mol Sci. 2023;24(10). https://doi.org/10.3390/ijms24108951.

76. Sen U, Coleman C, Sen T. Stearoyl coenzyme a desaturase-1: Multitasker in cancer, metabolism, and ferroptosis. Trends Cancer. 2023;9(6):480-9. https://doi.org/10.1016/j.trecan.2023.03.003.
77. Madison BB. Srebp2: A master regulator of sterol and fatty acid synthesis. J Lipid Res. 2016;57(3):333-5. https://doi.org/10.1194/jlr.C066712.
78. Xiong T, Xu G, Huang XL, Lu KQ, Xie WQ, Yin K, et al. Atp-binding cassette transporter a1: A promising therapy target for prostate cancer. Mol Clin Oncol. 2018;8(1):9-14. https://doi.org/10.3892/mco.2017.1506.
79. Pommier AJ, Alves G, Viennois E, Bernard S, Communal Y, Sion B, et al. Liver x receptor activation downregulates akt survival signaling in lipid rafts and induces apoptosis of prostate cancer cells. Oncogene. 2010;29(18):2712-23. https://doi.org/10.1038/onc.2010.30.
80. Jin Y, Tan Y, Wu J, Ren Z. Lipid droplets: A cellular organelle vital in cancer cells. Cell Death Discov. 2023;9(1):254. https://doi.org/10.1038/s41420-023-01493-z.
81. Fujimoto T, Parton RG. Not just fat: The structure and function of the lipid droplet. Cold Spring Harb Perspect Biol. 2011;3(3). https://doi.org/10.1101/cshperspect.a004838.
82. Zhang C, Liu P. The lipid droplet: A conserved cellular organelle. Protein Cell. 2017;8(11):796-800. https://doi.org/10.1007/s13238-017-0467-6.
83. Olzmann JA, Carvalho P. Dynamics and functions of lipid droplets. Nat Rev Mol Cell Biol. 2019;20(3):137-55. https://doi.org/10.1038/s41580-018-0085-z.
84. Cruz ALS, Barreto EA, Fazolini NPB, Viola JPB, Bozza PT. Lipid droplets: Platforms with multiple functions in cancer hallmarks. Cell Death Dis. 2020;11(2):105. https://doi.org/10.1038/s41419-020-2297-3.
85. Li J, Ren S, Piao HL, Wang F, Yin P, Xu C, et al. Integration of lipidomics and transcriptomics unravels aberrant lipid metabolism and defines cholesteryl oleate as potential biomarker of prostate cancer. Sci Rep. 2016;6:20984. https://doi.org/10.1038/srep20984.
86. Yue S, Li J, Lee SY, Lee HJ, Shao T, Song B, et al. Cholesteryl ester accumulation induced by pten loss and pi3k/akt activation underlies human prostate cancer aggressiveness. Cell Metab. 2014;19(3):393-406. https://doi.org/10.1016/j.cmet.2014.01.019.
87. Zaidi N, Lupien L, Kuemmerle NB, Kinlaw WB, Swinnen JV, Smans K. Lipogenesis and lipolysis: The pathways exploited by the cancer cells to acquire fatty acids. Prog Lipid Res. 2013;52(4):585-9. https://doi.org/10.1016/j.plipres.2013.08.005.
88. Melone MAB, Valentino A, Margarucci S, Galderisi U, Giordano A, Peluso G. The carnitine system and cancer metabolic plasticity. Cell Death and Disease. 2018;9(228):1-12. https://doi.org/10.1038/s41419-018-0313-7.
89. Ma Y, Zha J, Yang X, Li Q, Zhang Q, Yin A, et al. Long-chain fatty acyl-coa synthetase 1 promotes prostate cancer progression by elevation of lipogenesis and fatty acid beta-oxidation. Oncogene. 2021;40(10):1806-20. https://doi.org/10.1038/s41388-021-01667-y.
90. Valentino A, Calarco A, Di Salle A, Finicelli M, Crispi S, Calogero RA, et al. Deregulation of micrornas mediated control of carnitine cycle in prostate cancer: Molecular basis and pathophysiological consequences. Oncogene. 2017;36(43):6030-40. https://doi.org/10.1038/onc.2017.216.
91. Joshi M, Stoykova GE, Salzmann-Sullivan M, Dzieciatkowska M, Liebman LN, Deep G, et al. Cpt1a supports castration-resistant prostate cancer in androgen-deprived conditions. Cells. 2019;8(10). https://doi.org/10.3390/cells8101115.
92. Su YC, Feng YH, Wu HT, Huang YS, Tung CL, Wu P, et al. Elovl6 is a negative clinical predictor for liver cancer and knockdown of elovl6 reduces murine liver cancer progression. Sci Rep. 2018;8(1):6586. https://doi.org/10.1038/s41598-018-24633-3.
93. Grabner GF, Xie H, Schweiger M, Zechner R. Lipolysis: Cellular mechanisms for lipid mobilization from fat stores. Nat Metab. 2021;3(11):1445-65. https://doi.org/10.1038/s42255-021-00493-6.
94. Lytovchenko O, Kunji ERS. Expression and putative role of mitochondrial transport proteins in cancer. Biochim Biophys Acta Bioenerg. 2017;1858(8):641-54. https://doi.org/10.1016/j.bbabio.2017.03.006.
95. Hryb DJ, Nakhla AM, Kahn SM, St George J, Levy NC, Romas NA, et al. Sex hormone-binding globulin in the human prostate is locally synthesized and may act as an autocrine/paracrine effector. J Biol Chem. 2002;277(29):26618-22. https://doi.org/10.1074/jbc.M202495200.
96. Matsunaga T, Endo S, Maeda S, Ishikura S, Tajima K, Tanaka N, et al. Characterization of human dhrs4: An inducible short-chain dehydrogenase/reductase enzyme with 3beta-hydroxysteroid dehydrogenase activity. Arch Biochem Biophys. 2008;477(2):339-47. https://doi.org/10.1016/j.abb.2008.06.002.